Scientific Research Publishing

American Journal of Analytical Chemistry, 2024, 15, 201-218
https://www.scirp.org/journal/ajac
ISSN Online: 2156-8278
ISSN Print: 2156-8251

Mass-Based Environmental Factor and Energy Assessment of Microwave-Assisted Synthesized Transition Metal Nanostructures

Victor J. Law

School of Mechanical and Materials Engineering, University College Dublin, Dublin, Ireland
Email: viclaw66@gmail.com

How to cite this paper: Law, V.J. (2024) Mass-Based Environmental Factor and Energy Assessment of Microwave-Assisted Synthesized Transition Metal Nanostructures. *American Journal of Analytical Chemistry*, **15**, 201-218.
https://doi.org/10.4236/ajac.2024.156013

Received: May 14, 2024
Accepted: June 21, 2024
Published: June 24, 2024

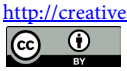

Abstract

This paper describes mass-based energy phase-space projection of microwave-assisted synthesis of transition metals (zinc oxide, palladium, silver, platinum, and gold) nanostructures. The projection uses process energy budget (measured in kJ) on the horizontal axes and process density (measured in $kJ \cdot g^{-1}$) on the vertical axes. These two axes allow both mass usage efficiency (Environmental-Factor) and energy efficiency to be evaluated for a range of microwave applicator and metal synthesis. The metrics are allied to the: second, sixth and eleventh principle of the twelve principle of Green Chemistry. This analytical approach to microwave synthesis (widely considered as a useful Green Chemistry energy source) allows a quantified dynamic environmental quotient to be given to renewable plant-based biomass associated with the reduction of the metal precursors. Thus allowing a degree of quantification of claimed "eco-friendly" and "sustainable" synthesis with regard to waste production and energy usage.

Keywords

Microwave-Assisted Synthesis, Transition Metals Nanostructures, Allometry Scaling, Power-Law Signature, Green Chemistry

1. Introduction

From the early 1960s, the lasting legacy of the American marine biologist, and author, Rachel Carson (1907-1964) has been to bring to an end the misuse of synthetic herbicides and pesticides by inspiring public opinion, then governments, to consider responsible protection of the environment (Carson (1962) [1]). The English scientist and environments James E Lovelock is best known for

developing the electron capture device that detects poisonous pesticides and the presence of chlorofluorocarbons that destroy the Earth's ozone layer (Lovelock, Maggs and Wades (1971) [2]), and the Gaia Hypothesis, which postulates that the Earth functions as a long term self-regulating system (Lovelock (1972) [3]) have become an important milestone in understanding the deleterious impact of human behavior on the Earth's biosphere. Perhaps the photograph of the Earth taken some 17,300 kilometer distance from the Earth by crew members of Apollo 17 spacecraft as it travelled to the moon (National Aeronautics and Space Administration (1972) [4] is generally acknowledged as one of the most influential images for the advocacy of Earths protection as it orbits through the Sun's heliosphere. In light of these examples, and surely many others, a new focus in chemical manufacture from one of pollution control and end-of-pipe waste treatment to one of pollution prevention began to be established. Initially described as "Minimum Impact Chemistry" (Drasar (1991) [5]), or "Benign by Design Chemistry" (Anastas (1994) [6]), this approach has many direct and indirect manufacturing cost benefits in various segments of the chemical industry. Now more formally known as "Green Chemistry" (Anastas and Warner (1998) [7]) it embodies the following twelve principles: 1) waste prevention not remediation, 2) reduce amount of material used (atom efficiency), 3) use benign (less harmful) materials, 4) safer products by design, 5) use less solvents and auxiliaries, 6) use less energy 7) use renewable feedstock (biomass), 8) reduce process time to produce less side-chain products, 9) use catalytic rather than stoichiometric reagents, 10) design products for degradation, 11) develop analytical methods for pollution control and finally, 12) use inherently safer processes.

Since the 1980s, microwave-assisted synthesis of organic compounds within microwave ovens (Gedye, Smith and Westaway (1988) [8], and Gedye, Rank and Westaway (1991) [9] have been found to encompass five of the twelve principles of Green Chemistry (use of fewer solvents and auxiliaries, use of less energy, reduced process time, and increased product yield). Following this a mass-based Environmental-Factor (E-Factor) metrics, or indicators (Sheldon (2008) [10], Sheldon (2018) [11], Abdussalam-Mohammeda, Alia and Errayes (2020) [12]), have been used to quantify the associated term "environmentally friendly, or benign" conditions that microwave applicators promote in the synthesis of organic compounds (Santra et al. (2014) [13]), and in transition metal complexes (Gabano and Ravera (2018) [14]). Recently (2023), it has been demonstrated that the E-Factors metrics can also be used to quantify and mitigate plastic waste and climate change (Sheldon (2023) [15]). Of further note, if all the material used in a chemical transformation is turned into useful products then there would be no waste, and the mass-based E-Factor would be of zero.

Recently, a historical review of forty-five microwave-assisted synthesis of Zinc oxide (ZnO), palladium (Pd), silver (Ag), platinum (Pt) and gold (Au) nanostructures and five dielectric volume heating of water (H_2O) exhibits a two-variable power-law signature ($y = 0.3293x^{0.846}$; $R^2 = 0.7923$) over four orders of magnitude (Law and Denis 2023) [16], Law and Denis (2023) [17], and

Law and Denis (2023) [18]) In this body the historical data (here termed **Database B**, n = 50) was mapped using process energy phase-space projection where the applied microwave energy (measured in kJ) is plotted on the horizontal axes and the process energy density (measured in $kJ \cdot ml^{-1}$) is plotted on the vertical axis. Using this means of projection a systematic energy efficiency index of the microwave-assisted synthesis allows a comparison to be made between different microwave applicator and chemical used, in the projection having a predictive value in designing new microwave synthesis pathways. However, there is a disconnect between established mass-based environmental metrics and the process energy density value that is measured in $kg \cdot ml^{-1}$ Thus there is a need to reevaluate the projection coordinates for full Green Chemistry integration.

The aim of this work is to remove the current disconnect between the initial process energy phase-space projection (where the energy density is volume-based) and mass-based E-Factor metrics. To achieve this aim, **Database B,** n = 50 is reexamined for the mass data. However, data mining across fifty different processes encounters many challenges (non-uniform method of reporting and recording of experimental data, or absent data), resulting in a reduction in usable information. To maintain the largest database as possible, a new search for alternative historical publications has been undertaken. This new database is called **Database C**, n = 49, see **Appendix 1**, Table A1. It is shown that using this new database a synergy between mass-based E-Factor metrics and the process energy phase-space projection enables a direct comparison of historical microwave-assisted synthesized transition metal nanostructures can be made. To further address environmental concerns plant-based biomass extract that contains natural bio-reducing agents that contribute to the overall reduction of the metal precursors is considered.

2. Methodology

2.1. Definition of Microwave Energy and Process Energy Density

The microwave power (Watts, $J \cdot s^{-1}$) from each historical publication and standardized in terms of process energy budget (Watts x process time to obtain kJ). The process energy density is obtained by diving the process energy budget by the mass of the suspension being irradiated and is calculated in $kJ \cdot g^{-1}$ [16] [17] [18].

2.2. Definition of E-Factor

Microwave-assisted synthesis of transition metal nanostructures process have been reported as either using a one-pot (facile) or a two-step process, where the nanostructure product is either carried in the facile process or in the second-step of the two-step process. In the first step or work-up step, conventional thermal or microwave energy is used to create the metal precursor and other reactants. As with estimating the energy within the microwave-assisted synthesis, the mass-based E-Factor calculation only considers the chemical used in the micro-

wave-assisted synthesis. This is the simplest E-Factor calculation possible, and here denoted as $E\text{-}F_m$ in Equation (1).

$$E\text{-}F_m = \text{waste/product, measured in grams} \quad (1)$$

In Equation (1), the numerator waste term contains the mass of the unused metal precursor, solvents and unconsumed reagents; and the denominator product contains the mass of the target metal nanostructure. In addition, the sum of waste mass and product mass equals the total mass of material used in the microwave-assisted reaction. Using this definition, the relatively vague adjectives "sustainable" and "eco" are outside this calculation and outside the scope of this work **Figure 1**. Indeed the chemical makeup of a nanostructure product that is intended to kill a target bacteria, fungi, or virus, may not be benign to non-targeted crustaceans, algae, and fish in the wider environment (Bondarenko *et al.* (2013) [19]).

Given that transition metal nanostructure product yields of 31% to 37% for ZnO (Cai and Hung (2023) [20], 50% to 88% for Pd supported on carbon frameworks (Rademacher *et al.* (2022) [21], and approximately 50% for Au (Putri, Pratiwi and Side (2021) [22]) have been reported, a target metal composition yield of 50% per metal precursor molar mass is assumed in all $E\text{-}F_m$ calculations. Where carbon frameworks are incorporated into the metal product a 50% carbon precursor mass usage is also assumed. Using these values it is implicit that the $E\text{-}F_m$ value never approaches zero. **Table 1** column 5.

2.3. Experimental Data Collection and High-Dimensional Space Spreadsheet Design

As with gathering and collating experimental data from different research sources, experimental reported is not reported in the same way, invariably leading to an incomplete database [16] [17] [18]. In this work **Database C**, n = 49, is collated from forty-one microwave-assisted synthesis of ZnO, Pd, Ag, Pt and Au

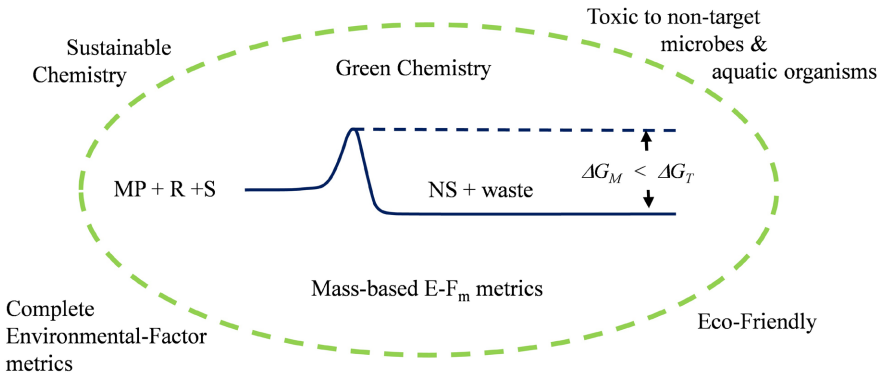

Figure 1. Chemical and energy flow plus mass-based $E\text{-}F_m$ metrics within the Green Chemistry domain. MP = metal precursor, R = reagents, S = solvents, and NS = nanostructure. ΔG_T and ΔG_m is the Gibbs free energy for thermal and microwave synthesis. Outside this domain can be found the terms relating to "sustainable chemistry" and "eco-friendly", and complete E-Factor metrics.

Table 1. Metal precursor chemical data (molar mass, density, and metal composition at 100% and 50% value.

Metal precursor	Molar mass ($g \cdot mol^{-1}$)	Density ($g \cdot cm^{-3}$)	100% metal percentage (g)	50% metal percentage (g)
$Zn(CH_3CO_2)_2 \cdot 2H_2O$	219.5	1.84	57.9	14.89
$ZnCl_2$	136.29	3.05	47.97	23.99
$Pd(C_5H_7O_2)_2$	304.64	1.96	35	17.50
$Pd(NO_3)_2$	230.42	3.54	46.18	23.09
$AgNO_3$	169.87	4.35	63.5	31.75
$H_2PtCl_6 \cdot xH_2O$	815.60	2.43	47.80	23.90
$HAuCl_4 \cdot xH_2O$	339.78	3.9	57.97	28.98

nanostructures publications [20]-[61] in which electrical-chemical synthesis data is reported. All synthesis except one continuous-flow mode operates the batch mode. The majority of the synthesis is performed in multi-mode microwave applicators (i.e. domestic microwave oven), where the sample is illuminated using a free running cavity magnetron operating a frequency of f_o = 2.45 ± 0.05 GHz (free wavelength, λ ~12.2 cm). The microwave applicators used in the **Database C**, n = 49 are: Microwave ovens, the CEM-Corporation Discover® 2.0 applicator (henceforth called the Discover® 2.0), the microwave ERTEC model 02-02, Wrocław-Poland applicator (henceforth called the ERTEC applicator) employs a sealed reaction vessel using in solvothermal (using a solvent other than H_2O at a moderate autogeneous pressure) nanostructure synthesis; temperature controlled microwave chemistry applicators (henceforth called TCMC applicator) that typically use a open to atmosphere reflux apparatus; Digestion applicators that use a sealed reaction vessel for solvothermal or hydrothermal (H_2O at moderate autogeneous pressure) nanostructures synthesis.

The electrical energy, time, and chemical information within **Database C**, n = 49 is collated using Microsoft Excel spread sheet software to generate a microwave-assisted high-dimensional dataset from which the data is dimensionally reduced for visualization as an XY scatter plot [62]. The data point facet (color size and shape) are used delineate the microwave applicator-type and target metal nanostructure as listed in Table 2. All microwave applicators operate in the batch-process mode, except one Discover 2.0 applicator that operates in the continuous-flow mode [58] and is denoted as a large (size 10) yellow filled triangle with black boarder. The six syntheses associated with renewable plant-based biomass are denoted with a large (size 10) green filled triangle or square with a black boarder.

The XY scatter plots use log-log transformation and linear regression power function trend-line fitted to the forty nine data to yield a two variable power-law signature that represents a 0-dimensional (0-D) model that does not give any underlying synthesis information Equation (2).

Table 2. Plot data-point facet (Color, size and shape) used to delineate microwave applicator-type and target transition metal nanostructure.

Applicator-type	Color and size	Target metal nanostructure	Shape
Microwave oven	Green (7)	ZnO	circle
Discover® 2.0 continuous-flow	Yellow (10)	Pd	star
Discover® batch-process	Yellow (7)	Ag	square
ERTEC-Poland	Black (7)	Pt	diamond
TCMC	Blue (7)	Au	triangle
Digestion	Red (7)		

$$y = cx^n \tag{2}$$

An overview of the weighting of each target metal product dataset is obtained by generating a linear regression fit trend-line Table 3 from which the constant c, exponent n and linear regression R^2 fit are obtained and evaluated.

3. Results

Figure 2 shows the log-log process energy phase-space projection of database C, n = 49. Log-log space is used here as the emphasis is on identifying a function over orders of magnitudes rather than outliers which can give a visually misleading illusion. Where the emphasis is the identification of outlier's log-linear space is generally used [18]. In this work, the Microsoft linear regression power function is used to calculate the least squares fit through the data points to obtain the trend-line $y = 0.007x^{1.1303}$; $R^2 = 0.5392$. The function splits the data into twenty above the trend-line, twenty three below the trend-line, and six points on the line. With regard to the applicator spread, the microwave oven (green) and TCMC Blue) applicators are spread across the length of the trend-line, the ERTEC applicators (black) are located high energy region, and finally the Discover® applicator operating in the continuous-flow mode used to synthesize Au rod-like nanostructures [58] (here denoted as a large yellow filled triangle with black boarder) is located at the extreme lower end (3.2 kJ) energy region. In contrast, the Discover® batch-process applicator used to synthesize Pd and Pd supported of carbon framework [21] are in the mid (120 kJ) energy region. In the mid energy range are the renewable plant-based biomass data points (large green triangle, square, and circle with black boarder). These data points are made from synthesized of Au nanostructure using white bol guava leaf extract [22]; synthesized ZnO using *Sandoricum koetjape* peel extract [32] [33]; synthesized of Ag from *Coleus amboinicus* leaf extract [39]; synthesized Ag using *Ocimum* leaf extract [47]; and synthesized Au using *Hibiscus rosa-sinensis* leaf extract [55].

Table 3 provides the Microsoft linear regression trend-line parameters (number of data points, slope intercept (c), exponent (n), and regression fit (R^2)). A simple

Table 3. Trend-line parameters for: ZnO, Pd, Ag, Pt, and Au nanostructures.

Metal	Data point #	*c*	*n*	R^2
ZnO	12	0.0018	1.2025	0.3572
Pd	6	0.012	1.1516	0.6016
Ag	14	0.012	1.1577	0.6905
Pt	4	6.916	0.5885	0.5139
Au	14	0.00006	1.1401	0.3858
Average of 5		1.3884	1.0140	0.5542
Average of 4 (minus Pt data)		0.0064	1.2787	0.5643

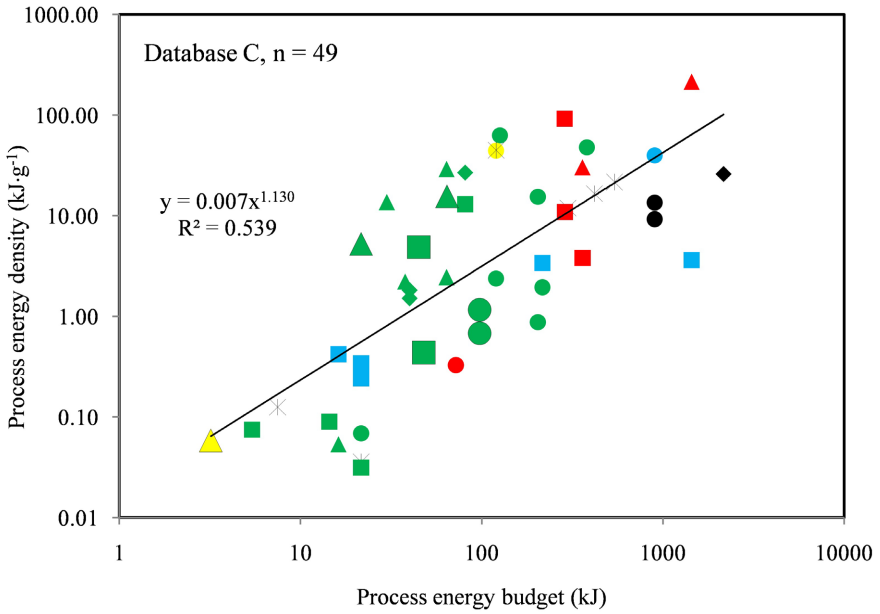

Figure 2. Log-log mass-based process energy phase-space projection. The Discover® 2.0 applicator operating in the continuous-flow mode is denoted as a large yellow triangle with black boarder. The plant-based biomass data points are denoted as large green triangles, squares circles with black borders. All other colors represent different microwave applicator types, and their shape represents different target metals.

statistical analysis of this data shows the average valve for *c* and *n*, and R^2 are: c = 1.3884 kJ·g^{-1}, n = 1.1406 and R^2 = 0.5542. Here it is noted that when evaluating a goodness of fit to a power-law using linear regression analysis, a low R^2 score is not necessary a good measure over two or more magnitudes of range [17] [63]. When removing the Pt data points from this average calculation (due to the low number of data point (4) and relative extreme value of *c*, a reduced average value of c = 0.064 kJ·g^{-1} and n = 1.2787 is obtained. Both of which are a close match to the power-law signature values observed in Figure 2. This outcome shows the need for evaluation tests when determining the contribution of subsets within a power-law signature.

To visualize the each term of Equation (1) a triplet rank plot is generated, where the magnitude and sign of the waste, product and E-F_m value are mapped

using a log scale to highlight the dynamic range of the calculated quantities. In general, the main attributes of this representation is twofold: first the extreme ends are candidates for outlier due to possible error in the data analysis and, second if the data is correct then low ranked data points will be associated with a large percentage of reactants transformed into product and high ranked data points with have a low percentage of reactants transformed into product. These two attributes therefore highlight possible uncertainties within the synthesis data, or if correct the "Greenness" of the synthesis within the data is easily identified.

Figure 3 shows this mapping operation using the same applicator-type color representation as in Figure 2, Table 2. For numerical ranked data see **Appendix 1**, Table A1. Using this representation the *E-F*$_m$ data forms a slow sign curve that increases in positive magnitude from 2.3 [48] to 4,583.7 [50]. There are four features of interest in the ranking. First, the TCMC microwave applicator-type (blue squares [25] [36] [43] [44] [45]) are gathered to the right of the ranking indicting that they are likely to generate more waste than products compared to other microwave applicator-types. This is because the applicator-type tends to use more solvents to produce the target product than the other applicator-types. Second, Pt products tend to be aligned in the middle (ranking: 16 to 24) using

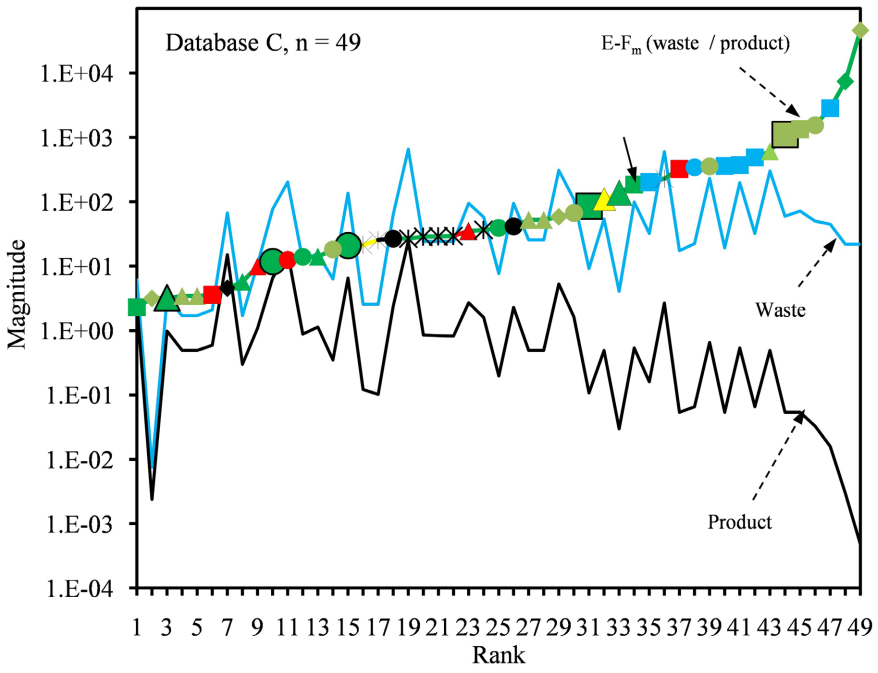

Figure 3. Triplet Rank plot: the different colored-line represents *E-F*$_m$ value for each microwave-assisted synthesis, solid black-line represents product mass value for each microwave-assisted synthesis, and light blue-line represents waste mass value for each microwave-assisted synthesis. The Discover® 2.0 applicator operating in the continuous-flow mode is denoted as a large yellow triangle with black boarder. The plant-based biomass extract data points are denoted as large green triangle, square and circle with black boarder. All other colors represent different microwave applicator-types, and their shape represents different target metals.

either the Discover® applicator operating in batch-process mode [21], or microwave oven applicators [34] [35] [54]. Third, the Discover® 2.0 applicator operating in the continuous-flow mode [58] is ranked 32. It is also noted that the Discover® 2.0 applicator operating in the continuous-mode to synthesize Au nano-rods has a higher $E\text{-}F_m$ value (109) when compared to its batch-process mode (21 to 25) which is used to synthesize Pd nanostructures. Fourth, a direct comparison can be made by comparing the two top ranking positions of 48 and 49, where the same microwave oven applicator is used to reduce hexachloroplatinate(IV) acid ($H_2PtCl_6{\cdot}xH_2O$) using ethylene glycol (EG) to form mono Pt nanoparticles, and Pt supported on a graphene framework [50]. Fifth, the six data points associated with plant-based biomass are spread out across the raking (3, 10, 15, 31, 33, and 44).

Of further note, the waste curve (light blue) and product curve (black) do not exhibit the smooth appearance of the $E\text{-}F_m$ data, but rather a mirrored irregular appearance is superimposed on their curves. This is because of the construct of the $E\text{-}F_m$ equation.

Figure 4 is a log-log $E\text{-}F_m$ process energy phase space projection of Database C, $n = 49$ where all the forty nine data points have a Microsoft fitted power function trend-line $y = 20711x^{-0.5}$; $R^2 = 0.1144$ which represents the scatter in the dataset. Nevertheless the exponent −0.5 reveals that $E\text{-}F_m$ tends to fall with process energy budget. The Discover® 2.0 applicator operating in continuous-flow has the lowest process energy budget (3.2 kJ) and a corresponding $E\text{-}F_m$ value of 109.82. With regard to the transition metal products that have been reduced using

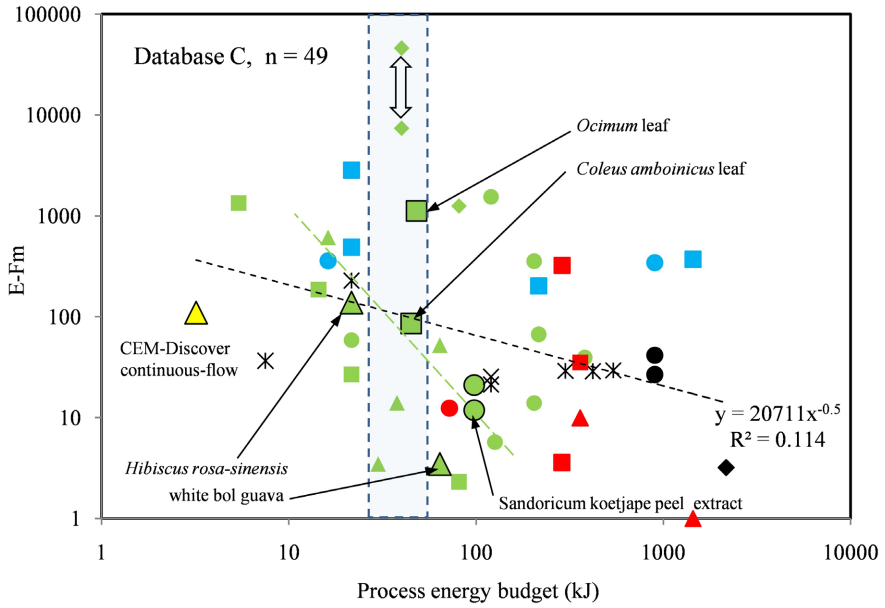

Figure 4. Log-log $E\text{-}F_m$ process energy phase-space projection. The Discover® 2.0 applicator operating in the continuous-flow mode is denoted as a large yellow triangle with black boarder. The plant-based biomass extract data points are denoted as large green triangles, squares, and circles with a black boarder. All other colors represent different microwave applicator-type, and their shape represents different target products.

plant-based biomass a meaningful way to assess two of them positioned within the projection is to examine a narrow process energy bandwidth (30 to 48 kJ) and then all six plant-based biomass data points in a broader process energy bandwidth (20 to 98 kJ) Table 4.

Within the narrow energy band the two highest rank $E\text{-}F_m$ values [50], the up-down arrow involves a one-pot reduction of $H_2PtCl_6{\cdot}xH_2O$ using EG to form mono Pt nanoparticles and Pt supported on graphene framework. In the case of the mono Pt nanopartcles, all of the reactants (expect the reduced Pt atoms that are transformed into the target product) are form in the numerator waste mass which appears of Equation (1). Conversely the part of graphene oxide (GO) is reduced to graphene that goes into the target metal product supporting framework, that is denominator term of Equation (1). Lastly, the un-reacted GO, released oxygen atoms and EG are formed in the numerator waste mass.

The mid range rank $E\text{-}F_m$ values microwave-assisted synthesis involves *Ocimum* leaf extract [39] and *Coleus amboinicus* leaf [47] extract to reduce silver nitrate ($AgNO_3$) to form mono Ag nanoparticles. In each case the synthesis is claimed to be "eco friendly" as renewable biomass is used in the synthesis.

The two lowest rank microwave-assisted synthesis $E\text{-}F_m$ values involve Sodium citrate (Na_3Ct) to reduce Chloroauric acid ($HAuCl_4{\cdot}3H_2O$) [59], and dimethyl sulfoxide (DMSO) to reduce Gold (III) chloride ($AuCl_3$) [56] to form mono Au nanoparticles. In these two cases the synthesis is claimed to be a "green" or "greener" approach to nanofabrication based on the use of microwave energy alone.

The six data points associated with renewable plant-based biomass have a Microsoft fitted power function trend-line $y = 1 \times 10^{11}x^{-2}$; $R^2 = 0.3032$ that crosses the 49 data points trend-line at 30 kJ and 107.7. These data points are made from synthesized of Au nanostructure using white bol guava leaf extract [22]; synthesized ZnO using *Sandoricum koetjape* peel extract [32] [33]; synthesized of Ag

Table 4. Narrow process energy bandwidth: process, waste, product, and $E\text{-}F_m$ values.

Applicator	Reactants	Product	Energy (kJ)	Waste (g)	Product (g)	$E\text{-}F_m$	Ref
Microwave oven	EG	Pt	40	22.00152	0.00048	45837.5	50
Microwave oven	EG GO	PtGo	40	22.00402	0.00298	7383.8	50
Microwave oven	*Ocimum* leaf extract	Ag	48	60.116	0.0538	1117.3	39
Microwave oven	*Coleus amboinicus* leaf extract	Ag	45	9.232	0.1077	85.72	47
Microwave oven	Na_3Ct	Au	37.8	15.869	1.131	14.02	59
Microwave oven	DMSO	Au	30	1.706	0.493	3.460	56

GO = graphene oxide, EG = ethylene glycol, Na_3Ct = Sodium citrate, and DMSO = dimethyl sulfoxide.

using *Coleus amboinicus* leaf extract [39]; synthesized Ag using *Ocimum* leaf extract [47]; and synthesized Au using *Hibiscus rosa-sinensis* leaf extract [56].

Today's environmental concerns encourages the use of renewable plant-based biomass in chemical reactions by attaching an environmental quotient to the environmental factor, the quotient represents the benign or non-benign nature of the waste [11]. Consequently, the $E\text{-}F_m$ values presented here need to be adjusted in some quantified way. The data presented in **Figure 4** and **Table 4** exhibits a dynamitic energy component when considering the process energy budget. For example, using a simple multiplying factor of 0.01 for [39] [47] would bring them in line with [56] [59] in the narrow energy band, but not outside this energy region. One way of achieving a quotient for all the plant-based biomass data points is to use the power-law function. For example, at 10 kJ a multiplying factor of 0.005 is used, and at 100 kJ a multiplying factor of 0.018 is used. It is important to note the quotient would be suitable for [22] [32] [33] and for [39] [47] as they deal with the reduction of $AgNO_3$ to form Ag nanostructure, the later when leached into the aquatic environment are toxic to crustaceans and protozoa [19].

4. Summary

This paper has constructed a mass-based process energy phase-space projection of microwave-assisted synthesis (widely considered as a useful Green Chemistry energy source) of transition metal (ZnO, Pd, Ag, Pt, and Au) nanostructures. The synthesis data has been obtained from forty-one publications published between 2004 and 2023. Using the reported chemical mass data (rather than volume data) and microwave power multiplied by process time ($J{\cdot}s^{-1} \times s = J$) of the synthesis, a simple environmental-factor ($E\text{-}F_m$ = waste measured in grams divided by product measured in grams) has been incorporated into the process energy phase-space projection. Collecting and collating the synthesis data is in line with the: second, sixth and eleventh principles of the twelve principles of Green Chemistry. Moreover, this analytical approach enables future microwave-assisted synthesis to be developed with the aim of reducing the amount of materials and energy consumed.

Highlights of this work are as follows:

Firstly, the using mass-based approach a power-law signature of $y = 0.0073x^{01.1303}$; $R^2 = 0.5932$ over three orders of magnitude is obtained. With an R^2 value of 0.5832 it can be postulated that the microwave energy transfer is directly proportional to the energy density ($kJ{\cdot}g^{-1}$). This differs from volume-based two variable sub-linear power-law signature $y = 0.3293x^{0.846}$; $R^2 = 0.7923$ over four orders of magnitude. Given that the transition metal precursors investigated here have a density ranging 2 to 13.9 $g{\cdot}ml^{-1}$ compared solvent investigated here (H_2O, EG, and ethanol) that are in the range of 1 to 1.2 $g{\cdot}ml^{-1}$, this may a have an important role in the 1/4 difference. However further investigation is required.

Secondly, rank plots have a useful role in revealing and exploring $E\text{-}F_m$ pro-

gression in regard to applicator-type the chemistry used.

Thirdly, as E-F_m metrics does not include an environmental impact of the generated waste (all waste is assigned the same environmental quotient), but for today's environmental concerns environmental quotient needs to be considered. In this work, it is shown that E-F_m falls with increasing process energy budget with an exponent −2. Using this dynamic reference it is proposed a plant-based biomass equivalent E-F_m to the best performing non-biomass syntheses of ZnO, Pd, Pt, and Au may be achieved by using a multiplying factor of 0.005 at 10 kJ, or 0.018 at 100 kJ. The use of this dynamic reference, should be used with caution when the synthesis process generates Ag nanostructures as they are known to have a toxic effect on crustaceans and protozoa.

Fourthly, by extension, the quotient process may be used for environmentally benign solvents. Where transition metals, such as Ag are present in the waste further work is required to identify a more robust environmental quotient factor.

Conflicts of Interest

The authors declare they have no conflicts of interest.

References

[1] Carson, R. (1962) Silent Spring. Houghton Mifflin Co.

[2] Lovelock, J.E., Maggs, R.J. and Wade, R.J. (1973) Halogenated Hydrocarbons in and over the Atlantic. *Nature*, **241**, 194-196. https://doi.org/10.1038/241194a0

[3] Lovelock, J.E. (1972) Gaia as Seen through the Atmosphere. *Atmospheric Environment* (1967), **6**, 579-580. https://doi.org/10.1016/0004-6981(72)90076-5

[4] NASA/Apollo 17 Crew. The Apollo 17 Full Earth Known as the Blue Marble. Source NASA, Flickr.com Project Apollo Archive. https://www.flickr.com/photos/projectapolloarchive

[5] Drasar, P. (1991) Green Chemistry—Dream or Reality (Minimum Impact Chemistry). *Chemické Listy*, **85**, 1144-1149.

[6] Anastas, P.T. (1994) Benign by Design Chemistry. In: Anastas, P.T. and Farris, C.A., Eds., *Benign by Design*: *Alternative Synthetic Design for Pollution Prevention*, ACS Symposium Series 577, American Chemical Society, 2-22.

[7] Anastas, P.T. and Warner, J.A. (1998) Green Chemistry: Theory and Practice. Oxford University Press.

[8] Gedye, R.N., Smith, F. and Westaway, K.C. (1988) The Rapid Synthesis of Organic Compounds in Microwave ovens. *Canadian Journal Chemistry*, **66**, 17-26.

[9] Gedye, R.N., Rank, W. and Westaway, K.C. (1991) The Rapid Synthesis of Organic Compounds in Microwave Ovens. II. *Canadian Journal Chemistry*, **69**, 706-711.

[10] Sheldon, R.A. (2008) E Factors, Green Chemistry and Catalysis: An Odyssey. *Chemical Communications*, **29**, 3352-3365. https://doi.org/10.1039/b803584a

[11] Sheldon, R.A. (2017) Metrics of Green Chemistry and Sustainability: Past, Present, and Future. *ACS Sustainable Chemistry & Engineering*, **6**, 32-48. https://doi.org/10.1021/acssuschemeng.7b03505

[12] Abdussalam-Mohammeda, W., Alia, A.Q. and Errayes, A.O. (2020) Green Chemi-

stry: Principles, Applications, and Disadvantages. *Chemical Methodologies*, **4**, 408-423.

[13] Santra, S., Rahman, M., Roy, A., Majee, A. and Hajra, A. (2014) Microwave-Assisted Three-Component "Catalyst and Solvent-Free" Green Protocol: A Highly Efficient and Clean One-Pot Synthesis of Tetrahydrobenzo[b]pyrans. *Organic Chemistry International*, **2014**, Article ID: 851924.

[14] Gabano, E. and Ravera, M. (2022) Microwave-Assisted Synthesis: Can Transition Metal Complexes Take Advantage of This "Green" Method? *Molecules*, **27**, Article No. 4249. https://doi.org/10.3390/molecules27134249

[15] Sheldon, R.A. (2023) The E Factor at 30: A Passion for Pollution Prevention. *Green Chemistry*, **25**, 1704-1728.

[16] Law, V.J. and Dowling, D.P. (2023) Microwave-Assisted Au and Ag Nanoparticle Synthesis: An Energy Phase-Space Projection Analysis. *American Journal of Analytical Chemistry*, **14**, 149-174. https://doi.org/10.4236/ajac.2023.144009

[17] Law, V.J. and Dowling, D.P. (2023) Microwave-Assisted Transition Metal Nanostructure Synthesis: Power-Law Signature Verification. *American Journal of Analytical Chemistry*, **14**, 326-349. https://doi.org/10.4236/ajac.2023.148018

[18] Law, V.J. and Dowling, D.P. (2023) Green Chemistry Allometry Test of Microwave-Assisted Synthesis of Transition Metal Nanostructures. *American Journal of Analytical Chemistry*, **14**, 493-518. https://doi.org/10.4236/ajac.2023.1411029

[19] Bondarenko, O., Juganson, K., Ivask, A., Kasemets, K. and Mortimer, M. (2013) Toxicity of Ag, CuO and ZnO Nanoparticles to Selected Environmentally Relevant Test Organisms and Mammalian Cells *in Vitro*: A Critical Review. *Archives of Toxicology*, **87**, 1181-1200.

[20] Cai, Y. and Huang, J. (2023) Preparation and Photocatalysis Characteristics of Flower-Like ZnO by Microwave Method. *Journal of Physics*: *Conference Series*, **2437**, Article ID: 012039. https://doi.org/10.1088/1742-6596/2437/1/012039

[21] Rademacher, L., Beglau, T.H.Y., Heinen, T., Barthel, J. and Janiak, C. (2022) Microwave-Assisted Synthesis of Iridium Oxide and Palladium Nanoparticles Supported on a Nitrogen-Rich Covalent Triazine Framework as Superior Electrocatalysts for the Hydrogen Evolution and Oxygen Reduction Reaction. *Frontiers in Chemistry*, **10**, Article No. 94526. https://doi.org/10.3389/fchem.2022.945261

[22] Putri, S.E., Pratiwi, D.E. and Side, S. (2021) The Effect of Microwave Irradiation on Synthesis of Gold Nanoparticles Using Ethanol Extract of White Bol Guava Leaves. *Journal of Physics*: *Conference Series*, **1752**, Article ID: 012058. https://doi.org/10.1088/1742-6596/1752/1/012058

[23] Cao, J., Wang, J., Fang, B., Chang, X., Zheng, M. and Wang, H. (2004) Microwave-Assisted Synthesis of Flower-Like ZnO Nanosheet Aggregates in a Room-Temperature Ionic Liquid. *Chemistry Letters*, **33**, 1332-1333. https://doi.org/10.1246/cl.2004.1332

[24] Cao, Y., Liu, B., Huang, R., Xia, Z. and Ge, S. (2011) Flash Synthesis of Flower-Like ZnO Nanostructures by Microwave-Induced Combustion Process. *Materials Letters*, **65**, 160-163. https://doi.org/10.1016/j.matlet.2010.09.072

[25] Li, X., Wang, C., Zhou, X., Liu, J., Sun, P. and Lu, G. (2014) Gas Sensing Properties of Flower-Like ZnO Prepared by a Microwave-Assisted Technique. *RSC Advances*, **4**, 47319-47324. https://doi.org/10.1039/c4ra07425d

[26] Hasanpoor, M., Aliofkhazraei, M. and Delavari, H. (2015) Microwave-Assisted Synthesis of Zinc Oxide Nanoparticles. *Procedia Materials Science*, **11**, 320-325. https://doi.org/10.1016/j.mspro.2015.11.101

[27] Krishnapriya, R., Praneetha, S. and Murugan, A.V. (2016) Investigation of the Effect of Reaction Parameters on the Microwave-Assisted Hydrothermal Synthesis of Hierarchical Jasmine-Flower-Like ZnO Nanostructures for Dye-Sensitized Solar Cells. *New Journal of Chemistry*, **40**, 5080-5089. https://doi.org/10.1039/c6nj00457a

[28] Wojnarowicz, J., Opalinska, A., Chudoba, T., Gierlotka, S., Mukhovskyi, R., Pietrzykowska, E., *et al*. (2016) Effect of Water Content in Ethylene Glycol Solvent on the Size of ZnO Nanoparticles Prepared Using Microwave Solvothermal Synthesis. *Journal of Nanomaterials*, **2016**, Article ID: 2789871. https://doi.org/10.1155/2016/2789871

[29] Wojnarowicz, J., Chudoba, T., Gierlotka, S., Sobczak, K. and Lojkowski, W. (2018) Size Control of Cobalt-Doped ZnO Nanoparticles Obtained in Microwave Solvothermal Synthesis. *Crystals*, **8**, Article No. 179.

[30] Liu, H., Liu, H., Yang, J., Zhai, H., Liu, X. and Jia, H. (2019) Microwave-Assisted One-Pot Synthesis of Ag Decorated Flower-Like ZnO Composites Photocatalysts for Dye Degradation and NO Removal. *Ceramics International*, **45**, 20133-20140. https://doi.org/10.1016/j.ceramint.2019.06.279

[31] 1] Aljaafari, A., Ahmed, F., Awada, C. and Shaalan, N.M. (2020) Flower-Like ZnO Nanorods Synthesized by Microwave-Assisted One-Pot Method for Detecting Reducing Gases: Structural Properties and Sensing Reversibility. *Frontiers in Chemistry*, **8**, Article No. 456. https://doi.org/10.3389/fchem.2020.00456

[32] Rini, A.S., Rati, Y. and Maisita, S.W. (2021) Of ZnO Nanoparticle Using Sandoricum Koetjape Peel Extract as Bio-Stabilizer under Microwave Irradiation. *Journal of Physics*: *Conference Series*, **2049**, Article ID: 012069. https://doi.org/10.1088/1742-6596/2049/1/012069

[33] Sulistyo Rini, A., Aji, A.P. and Rati, Y. (2022) Microwave-Assisted Biosynthesis of Flower-Shaped ZnO for Photocatalyst in 4-Nitrophenol Degradation. *Communications in Science and Technology*, **7**, 135-139. https://doi.org/10.21924/cst.7.2.2022.937

[34] Elazab, H.A., Moussa, S., Gupton, B.F. and El-Shall, M.S. (2014) Microwave-Assisted Synthesis of Pd Nanoparticles Supported on Fe_3O_4, Co_3O_4, and $Ni(OH)_2$ Nanoplates and Catalysis Application for CO Oxidation. *Journal of Nanoparticle Research*, **16**, Article ID: 2477. https://doi.org/10.1007/s11051-014-2477-0

[35] Elazab, H.A., Sadek, M.A. and El-Idreesy, T.T. (2018) Microwave-Assisted Synthesis of Palladium Nanoparticles Supported on Copper Oxide in Aqueous Medium as an Efficient Catalyst for Suzuki Cross-Coupling Reaction. *Adsorption Science & Technology*, **36**, 1352-1365. https://doi.org/10.1177/0263617418771777

[36] Chen, J., Wang, J., Zhang, X. and Jin, Y. (2008) Microwave-Assisted Green Synthesis of Silver Nanoparticles by Carboxymethyl Cellulose Sodium and Silver Nitrate. *Materials Chemistry and Physics*, **108**, 421-424.

[37] Blosi, M., Albonetti, S., Gatti, F., Dondi, M., Migliori, A., Ortolani, L., Morandi, V. and Baldi, G. (2010) Au, Ag and Au-Ag Nanoparticles: Microwave-Assisted Synthesis in Water and Applications in Ceramic and Catalysis. *Nanotech*, **1**, 352-355.

[38] Wang, B., Zhuang, X., Deng, W. and Cheng, B. (2010) Microwave-Assisted Synthesis of Silver Nanoparticles in Alkalic Carboxymethyl Chitosan Solution. *Engineering*, **2**, 387-390.

[39] Saha, S., Malik, M.M. and Qureshi, M.S. (2013) Microwave Synthesis of Silver Nanoparticles. *Nano Hybrids*, **4**, 99-112. https://doi.org/10.4028/www.scientific.net/nh.4.99

[40] Iqbal, N., Abdul Kadir, M.R., Nik Malek, N.A.N., Mahmood, N.H.B., Murali, M.R. and Kamarul, T. (2013) Characterization and Antibacterial Properties of Stable Silver Substituted Hydroxyapatite Nanoparticles Synthesized through Surfactant Assisted Microwave Process. *Materials Research Bulletin*, **48**, 3172-3177. https://doi.org/10.1016/j.materresbull.2013.04.068

[41] Pal, J., Deb, M.K. and Deshmukh, D.K. (2013) Microwave-Assisted Synthesis of Silver Nanoparticles Using Benzo-18-Crown-6 as Reducing and Stabilizing Agent. *Applied Nanoscience*, **4**, 507-510. https://doi.org/10.1007/s13204-013-0229-6

[42] Rai, P., Majhi, S.M., Yu, Y. and Lee, J. (2015) Synthesis of Plasmonic Ag@SnO_2 Core-Shell Nanoreactors for Xylene Detection. *RSC Advances*, **5**, 17653-17659. https://doi.org/10.1039/c4ra13971b

[43] Karimipour, M., Mollaei, M., Shabani, E., Molaei, M., Ashrafi, J. and Saghatoleslami, N. (2015) Microwave Synthesis of Oleylamine-Capped Ag Nanoparticles in Aqueous Solution. *Materials Science*, **21**, 182-186. https://doi.org/10.5755/j01.ms.21.2.6480

[44] Ebrahimi, M., Zakery, A., Karimipour, M. and Molaei, M. (2016) Nonlinear Optical Properties and Optical Limiting Measurements of Graphene Oxide-Ag@TiO_2 Compounds. *Optical Materials*, **57**, 146-152. https://doi.org/10.1016/j.optmat.2016.04.039

[45] Karimipour, M., Mostoufirad, S., Molaei, M., Nikabadi, H.R. and Nesheli, A.G. (2016) Free Reducing Agent, One Pot, and Two Steps Synthesis of Ag@SiO_2 Core-Shells Using Microwave Irradiation. *Journal of Nano- and Electronic Physics*, **8**, Article No. 03020. https://doi.org/10.21272/jnep.8(3).03020

[46] Miglietta, M.L., Alfano, B., Polichetti, T., Massera, E., Schiattarella, C. and Francia, G.D. (2018) Effective Tuning of Silver Decorated Graphene Sensing Properties by Adjusting the Ag NPs Coverage Density. *Sensors*: *Proceedings of the Third National Conference on Sensors*, Rome, 23-25 February 2016.

[47] Jyothi, D., Cherriyan, S.P., Ahmed, S.R.R., Priya, S., *et al.* (2020) Microwave Assisted Green Synthesis of Silver Nanoparticles Using Coleus Amboinicus Leaf Extract. *International Journal of Applied Pharmaceutics*, **12**, 56-61.

[48] Ahmed, F., AlOmar, S.Y., Albalawi, F., Arshi, N., Dwivedi, S., Kumar, S., *et al.* (2021) Microwave Mediated Fast Synthesis of Silver Nanoparticles and Investigation of Their Antibacterial Activities for Gram-Positive and Gram-Negative Microorganisms. *Crystals*, **11**, Article No. 666. https://doi.org/10.3390/cryst11060666

[49] Li, D. and Komarneni, S. (2006) Synthesis of Pt Nanoparticles and Nanorods by Microwave-Assisted Solvothermal Technique. *Zeitschrift fuer Naturforschung B*, **61**, 1566-1572.

[50] Kundu, P., Nethravathi, C., Deshpande, P.A., Rajamathi, M., Madras, G. and Ravishankar, N. (2011) Ultrafast Microwave-Assisted Route to Surfactant-Free Ultrafine Pt Nanoparticles on Graphene: Synergistic Co-Reduction Mechanism and High Catalytic Activity. *Chemistry of Materials*, **23**, 2772-2780. https://doi.org/10.1021/cm200329a

[51] Pal, J., Deb, M.K., Deshmukh, D.K. and Sen, B.K. (2014) Microwave-Assisted Synthesis of Platinum Nanoparticles and Their Catalytic Degradation of Methyl Violet in Aqueous Solution. *Applied Nanoscience*, **4**, 61-65.

[52] Wojnicki, M., Luty-Błocho, M., Kwolek, P., Gajewska, M., Socha, R.P., Pędzich, Z., *et al.* (2021) The Influence of Dielectric Permittivity of Water on the Shape of Ptnps Synthesized in High-Pressure High-Temperature Microwave Reactor. *Scientific Reports*, **11**, Article No. 4851. https://doi.org/10.1038/s41598-021-84388-2

[53] Liu, F.K., Huang, P.W., Chang, Y.C., Ko, C.J., Ko, F.H. and Chu, T.C. (2005) Formation of Silver Nanorods by Microwave Heating in the Presence of Gold Seeds. *Journal of Crystal Growth*, **273**, 439-445.

[54] Mallikarjuna, N.N. and Varma, R.S. (2017) Microwave-Assisted Shape-Controlled Bulk Synthesis of Noble Nanocrystals and Their Catalytic Properties. *Crystal Growth & Design*, **8**, 291-295.

[55] Yasmin, A., Ramesh, K. and Rajeshkumar, S. (2014) Optimization and Stabilization of Gold Nanoparticles by Using Herbal Plant Extract with Microwave Heating. *Nano Convergence*, **1**, 12.

[56] Bhosale, M.A., Chenna, D.R., Ahire, J.P. and Bhanage, B.M. (2015) Morphological Study of Microwave-Assisted Facile Synthesis of Gold Nanoflowers/Nanoparticles in Aqueous Medium and Their Catalytic Application for Reduction of p-Nitrophenol to p-Aminophenol. *Royal Society of Chemistry Advances*, **5**, 52817-52823.

[57] Ngo, V.K.T., Nguyen, H.P.U., Huynh, T.P., Tran, N.N.P., Lam, Q.V. and Huynh, T.D. (2015) Preparation of Gold Nanoparticles by Microwave Heating and Application of Spectroscopy to Study Conjugate of Gold Nanoparticles with Antibody *E. coli* O157:H7. *Advances in Natural Sciences: Nanoscience and Nanotechnology*, **6**, Article ID: 035015. https://doi.org/10.1088/2043-6262/6/3/035015

[58] Bayazit, M.K., Yue, J., Cao, E., Gavriilidis, A. and Tang, J. (2016) Controllable Synthesis of Gold Nanoparticles in Aqueous Solution by Microwave Assisted Flow Chemistry. *ACS Sustainable Chemistry & Engineering*, **4**, 6435-6442. https://doi.org/10.1021/acssuschemeng.6b01149

[59] Shah, K.W. and Zheng, L. (2019) Microwave-Assisted Synthesis of Hexagonal Gold Nanoparticles Reduced by Organosilane (3-Mercaptopropyl)trimethoxysilane. *Materials*, **12**, Article No. 1680. https://doi.org/10.3390/ma12101680

[60] Marinoiu, A., Andrei, R., Vagner, I., Niculescu, V., Bucra, F., Constantinescu, M. and Carcadea, E. (2020) One Step Synthesis of Au Nanoparticles Supported on Graphene Oxide Using an "Eco-Friendly" Microwave-Assisted Process. *Materials Science*, **26**, 249-254.

[61] Ngo, V.K.T., Nguyen, D.G., Huynh, T.P. and Lam, Q.V. (2016) A Low Cost Technique for Synthesis of Gold Nanoparticles Using Microwave Heating and Its Application in Signal Amplification for Detecting *Escherichia coli* O157:H7 Bacteria. *Advances in Natural Sciences: Nanoscience and Nanotechnology*, **7**, Article ID: 035016. https://doi.org/10.1088/2043-6262/7/3/035016

[62] Liu, S., Maljovec, D., Wang, B., Bremer, P.T. and Pascucci, V. (2017) Visualizing High-Dimensional Data: Advances in the Past Decade. *IEEE Transaction on Visualization and Computer Graphs*, **23**, 21.

[63] Stumpf, M.P.H. and Porter, M.A. (2012) Critical Truths about Power Laws. *Science*, **335**, 665-666. https://doi.org/10.1126/science.1216142

Appendix 1

Table A1. Database C, $n = 49$; $E\text{-}F_m$ ranked data.

Reference	First author	Date	Applicator	Target Metal	Waste	Product	$E\text{-}F_m$
48	Ahmed	2021	MO	Ag	6.201166	2.692489	2.303136
51	Pal	2014	MO	Pt	0.0076	0.0024	3.166667
22	*Purti*	*2019*	*MO*	*Au*	*3.146161*	*0.978714*	*3.214588*
56	Bhosale	2015	MO	Au	1.706237	0.492688	3.463116
57	Bhosale	2015	MO	Au	1.706237	0.492688	3.463116
46	Miglietta	2018	Digestion	Ag	2.110233	0.588498	3.585797
52	Wojnicki	2001	ERTEC	Pt	67.87324	14.95488	4.538535
23	Cao	2004	MO	Au	1.7022	0.2978	5.715917
37	Blosi	2010	Digestion	Au	10.77525	1.083914	9.941054
33	*Rini*	*2022*	*MO*	*ZnO*	*77.36159*	*6.536412*	*11.83548*
27	Krishnapriya	2016	Digestion	ZnO	203.154	16.34103	12.43214
24	Cao	2011	MO	ZnO	12.29848	0.882416	13.93728
59	Shah	2019	MO	Au	15.869	1.131	14.03095
60	Marinoiu	2020	Digestion	Au	6.37	0.35	18.2
32	*Rini*	*2021*	*MO*	*ZnO*	*137.3616*	*6.536412*	*21.01483*
21	Rademacher	2022	Discover®	Pd	2.5792	0.12136	21.25247
21	Rademacher	2022	Discover®	Pd	2.5792	0.10136	25.44594
29	Wojnarowicz	2018	ERTEC	ZnO	64.0729	2.397104	26.72929
54	Mallikarjuna	2017	MO	Pd	660.305	24.6316	26.80723
34	Elazab	2014	MO	Pd	24.40132	0.848463	28.75943
34	Elazab	2014	MO	Pd	24.28622	0.83613	29.04598
34	Elazab	2014	MO	Pd	24.28622	0.826266	29.39273
37	Blosi	2010	Digestion	Au	94.65329	2.692489	35.15457
35	Elazab	2018	MO	Pd	58.07924	1.588417	36.56424
26	Hasanpoor	2015	MO	ZnO	7.720848	0.196092	39.37352
27	Wojnarowicz	2016	ERTEC	ZnO	94.9729	2.287104	41.52539
57	Ngo	2015	MO	Au	25.65774	0.492688	52.07702
61	Ngo	2016	MO	Au	25.65774	0.492688	52.07702
54	Mallikarjuna	2017	MO	Pt	308.2347	5.264805	58.54627
31	Aljaafari	2020	MO	ZnO	109.3404	1.634103	66.91157
47	*Jyothi*	*2020*	*MO*	*Ag*	*9.232047*	*0.1077*	*85.72039*
58	Bayazit	2016	*Discover®	Au	54.10924	0.492688	109.8245
55	*Yasmin*	*2014*	*MO*	*Au*	*4.072374*	*0.029561*	*137.7603*
38	Wang	2010	MO	Ag	99.86023	0.538498	185.4423

Continued

45	Karimipour	2016	TCMC	Ag	32.32843	0.160127	201.8922
54	Mallikarjuna	2007	MO	Pd	606.2064	2.65989	227.9066
53	Liu	2005	Digestion	Ag	17.41772	0.05385	323.4503
25	Li	2014	TCMC	ZnO	22.47448	0.065516	343.0381
20	Cai	2023	MO	ZnO	232.0718	0.6539	354.904
43	Karimipour	2015	TCMC	Ag	19.31772	0.05385	358.7336
35	Chen	2008	TCMC	Ag	199.4612	0.538498	370.4031
44	Karimipour	2016	TCMC	Ag	32.18415	0.06585	488.7494
53	Mallikarjuna	2007	MO	Au	301.2062	0.492688	611.3526
38	*Saha*	*2013*	*MO*	*Ag*	*60.11602*	*0.05385*	*1116.365*
40	Pal	2014	MO	Ag	72.19722	0.05385	1340.715
29	Liu	2019	MO	ZnO	50.42675	0.032682	1542.949
43	Ebrahimi	2016	TCMC	Ag	45.03415	0.01585	2841.271
49	Kundu	2011	MO	PtGO	22.00402	0.00298	7383.899
49	Kundu	2011	MO	Pt	22.00152	0.00048	45836.5